A Comparative Study: Predictive Modeling of Wind Turbine Blades

Kendra L. Van Buren*, and Sez Atamturktur†
Department of Civil Engineering, Clemson University, Clemson, SC 29634

Submitted June 7, 2011; Revised March 27, 2012, Accepted May 30, 2012.

ABSTRACT

The structural analysis of wind turbine blades is completed using vastly different computational modeling strategies with varying levels of model sophistication and detail. Typically, preference of one modeling strategy over the other is decided according to subjective judgment of the expert. The central question that arises is how to justify the chosen level of sophistication and detail through quantitative, objective and scientifically defendable metrics. This manuscript takes a step toward answering this question and investigates the necessary level of sophistication and detail needed while modeling the cross-section of wind turbine blades by: i) rigorously quantifying the *model incompleteness* resulting from simplifying assumptions and ii) comparing the predictive maturity index associated with alternative modeling strategies. The concept of predictive maturity is illustrated on a prototype blade. The incompleteness of five alternative models with varying sophistication in the cross section of the shell elements are assessed through *model form error and predictive maturity index*. While model form error is observed as constant for varying levels of sophistication, through the predictive maturity index, it is found that models with lesser sophistication may have predictive capabilities comparable to more sophisticated, computationally expensive models.

1. INTRODUCTION

In the United States, wind energy has the potential to supply 20% of energy capacity by 2030 [1]. Wind plants, and the wind turbines comprising those plants, are being produced at an increasingly greater scale to capture and produce more energy to meet the growing demands of the wind energy industry [2, 3]. To ensure our reliance upon current sources of wind energy and the expansion of this nascent technology, it is crucial to understand the dynamics of wind turbine blades, which are the first to extract energy from the wind and generate all loads on the system [4, 5, 6, 7]. Though wind turbine blades account for only 10–15% of the cost of the wind turbine system [2], subsequent damage can result in rotor instability and damage to the entire system [8]. Full scale testing is essential for studying the performance of wind turbine blades, however, is limited to providing measurements of the response due to idealized loads, and becomes more expensive as wind turbine blades are produced at a larger scale [2].

Recently, modeling and simulation (M&S) has become a widely accepted approach for the study and analysis of wind turbine blades, owing to their versatility in predicting many complex load cases that are impractical to implement in laboratory settings [9]. Further, M&S techniques have become commonplace in design standards and certifications [10], offering a

*Corresponding author, Email : Ph.D Candidate, klvan@clemson.edu, †Assistant Professor, sez@clemson.edu

cost and time efficient alternative for the study and analysis of wind turbines. Reliance on M&S in the study of wind turbine blades has been established for the study of innovative designs [6, 11], structural health monitoring techniques [12, 13], and potential power output when coupled with computational fluid dynamics models [14, 15, 16]. It must be emphasized however that M&S, while elaborate, only supplies an approximation of reality. Therefore, there is a need to quantify the incompleteness of numerical models and establish guidelines for the level of sophistication and detail necessary for achieving the desired accuracy in wind turbine blade modeling. This manuscript takes a step in this direction and quantifies the model incompleteness through model form error [17].

This manuscript investigates the degrading effects of modeling simplifications on the predictive maturity of finite element (FE) models of a 44-meter prototype wind turbine blade. The modeling simplification investigated herein comes from the reduced detail in the cross-section of the blade. The most sophisticated model (henceforth referred to as the *baseline model*) is built with orthotropic materials and a composite cross-section, requiring 90 material dependent input parameters, while the least sophisticated model is built with an isotropic, smeared cross-section, needing only 20 input parameters. The simplifications to the material cross-sections affect not only the *model form error* due to model incompleteness but also the number of input parameters. Hence, a central question of interest is whether the increased number of material dependent input parameters, and thus the uncertainty in prediction, is justified by the gain in the predictive maturity, i.e. reduced model form error.

This manuscript is motivated by the evidence found in pertinent literature regarding the lack of uniformity in the development of FE models of wind turbine blades, see Section 2.1. In Section 2.2, we introduce concepts essential to the approach implemented for quantifying the model incompleteness of numerical models. In Section 2.3, a proof of concept example is provided that discusses the effect of model form error on predictiveness of numerical models. In Section 3.1, we overview the development of alternative FE models of the prototype blade used in this study. Verification studies, necessary to ensure that estimates of model form error are not contaminated with numerical errors, are discussed in Section 3.2. In Section 4, the model form error associated with simplified, less-sophisticated FE models is evaluated. Section 5 goes a step further and implements the predictive maturity index (PMI), a quantitative metric that supplies a holistic assessment of the predictive capabilities of numerical models. Section 6 provides a discussion of findings, an overview of the underlying premises, and the limitations of the presented approach.

2. BACKGROUND

M&S offers a faster and more economical alternative to building and testing blades during the design phase. This, however, introduces a new paradigm of how to create accurate predictive models for wind turbine blades. Consequently, a cursory review of efforts in M&S of wind turbine blades is provided in Section 2.1. Model form error, a concept essential to this paper, is introduced in Section 2.2 and demonstrated with a proof of concept example in Section 2.3.

2.1. Review of pertinent literature

In the pertinent literature, diverse modeling strategies have been implemented to study the behavior of wind turbine blades. For instance, Ref. [18] claimed shell and brick elements in a linear analysis to provide sufficiently accurate predictions, while another study found it necessary to use a non-linear analysis [19]. Often, reducing the computational cost of the analysis has been pursued through the use of one-dimensional beam elements to represent three-dimensional effects [20], or by non-linear composite laws to smear the cross section and

leave out unnecessary details provided by micromechanical models [21]. Modeling strategies specifically for wind turbine blades have also been proposed, such as new element formulations for the FE analysis [22], or the use of reduced-order analysis methods to forgo the FE method [23].

Undeniably, different modeling strategies change the number of input parameters that need to be accurately defined to reach high-fidelity solutions. Of course, keeping the number of parameters low makes the sensitivity analysis, uncertainty quantification and accompanying calibration activities manageable. Moreover, increased number of uncertain input parameters may very well increase the uncertainty in the model predictions. Therefore, there is a trade-off between increasing the model sophistication and detail and managing the uncertainties associated with the model development.

Earlier studies have completed qualitative comparisons of the predictiveness of alternative modeling strategies. For instance, Ref. [24] compared the performance of shell and solid models to evaluate the response of a box girder of a wind turbine blade to compressive loads. Both shell and solid models used in the study were deemed sufficient, except that shell elements were unable to model geometric non-linearity when deflections were comparable to the laminate thickness. Ref. [7] investigated the tradeoffs of 2-dimensional analysis versus 3-dimensional analysis. Equivalent beam properties were extracted for blade models developed using both techniques, with the 3-dimensional approach producing a more flexible result. In addition to this qualitative assessment, the authors suggest that the ease in which a 2-dimensional analysis can be performed is appropriate for preliminary design, while 3-dimensional models are necessary for more detailed investigations of blades. This present study supplies a unique contribution to the existing literature as it illustrates an *objective, scientifically defendable* and *quantitative* comparison between alternative modeling strategies for wind turbine blades.

2.2 Model form error

Model form error is defined as the difference between physical reality and model predictions that cannot be further reduced via parameter calibration and in this study, is estimated as proposed in Ref. 17 (Eqn. 1):

$$y_{obs}(x) = y_{sim}(x;\theta) + \delta(x) + \varepsilon^{Test} \tag{1}$$

where $y_{obs}(x)$ are the physical or observed measurements, $y_{sim}(x;\theta)$ are the model predictions, $\delta(x)$ is the discrepancy term, and ε^{Test} is the measurement error. In Eqn. 1, x represents control parameters, which are factors that can be controlled during an experiment. These parameters define the domain within which the model is expected to make accurate predictions. The calibration parameters are represented by θ, which are parameters that are input to the model but not observed during experimentation.

In reality, model form error is only known at discrete settings where experiments are available and thus, must be estimated for untested settings. Herein, discrepancy is estimated using a fully Bayesian interpretation as proposed by Ref. 25. Our best estimate of model form error is obtained by training a Gaussian Process Model (GPM) and referred to as *discrepancy bias*.

2.3. Model sophistication: proof of concept

This section presents a simple proof of concept example to demonstrate model incompleteness as presented in Ref. 26. First, we define an arbitrary mathematical function referred to as "truth".

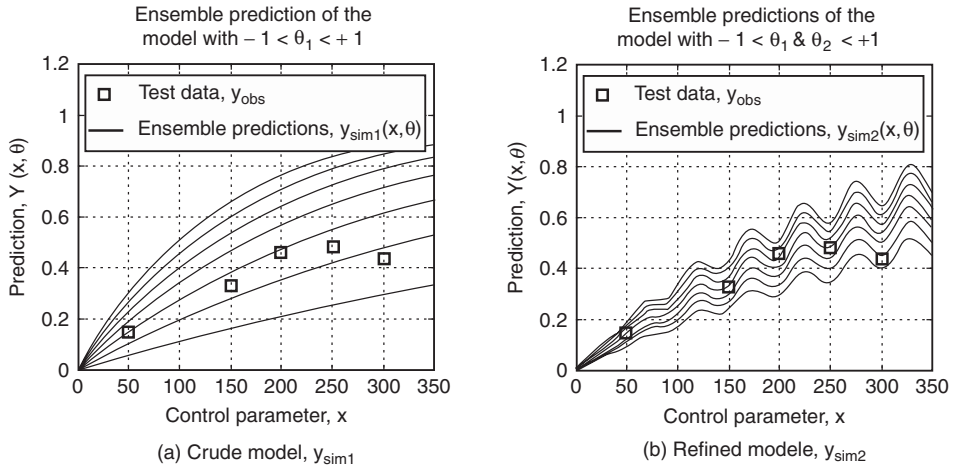

Figure 1: Ensemble plots of the model predictions.

We randomly select five control parameter values, x, and generate synthetic observations using the truth function (see Figure 1a). Next, from the same truth function, two *incomplete* simulation models are derived by incrementally reducing the number of mathematical terms. Here, we discuss the predictive capabilities of these two distinct models with different levels of model sophistication: crude model (y_{sim1}) and a refined model (y_{sim2}).

The crude model, y_{sim1}, has only one uncertain input parameter, θ_1, which is known to have a value between 0 and 1. Figure 1a shows an ensemble of crude model predictions obtained by varying θ_1 within its upper and lower limits. The ensemble predictions of this crude model are unable to reproduce all five experimental observations. This inability is because the mathematical function for y_{sim1} is lacking essential terms (and thus essential input parameters) that are present in the truth function. Such incompleteness results in discrepancy bias, δ_{y1}.

The refined model, y_{sim2} has additional mathematical terms, which result in an additional input parameter, θ_2. By allowing both θ_1 and θ_2 to vary within their predefined ranges, a new ensemble of refined model predictions can be obtained as shown in Figure 1b. Although improved in its model sophistication, the refined model (y_{sim2}) is still incomplete and has an associated discrepancy bias, δ_{y2}.

Figure 2 presents the mean of ensemble predictions for y_{sim1} and y_{sim2}, along with the corresponding plots for discrepancy bias, $\delta_{y1}(x)$ and $\delta_{y2}(x)$. The improvement in predictive abilities of the second model can be visually observed in Figure 2, wherein the function of the refined model, y_{sim2}, is able to better capture the behavior of the truth function compared to y_{sim1}.

The increased sophistication of model y_{sim2} allows for a reduction in discrepancy and more adequate predictions of synthetic observations. However, the fact that y_{sim2} has more uncertain input parameters compared to y_{sim1} cannot be overlooked as more uncertain parameters may translate to more uncertainty in the predictions.

3. MODEL DEVELOPMENT AND VERIFICATION

In this section, the development and verification of the FE models are discussed. Verification studies are especially important for this study, since numerical errors, if not controlled, can contaminate the predictions of model form error.

3.1. Model development with NuMAD

NuMAD, pre-processing software developed at Sandia National Laboratories, is utilized to create the three-dimensional FE model of a prototype wind turbine blade with Shell281

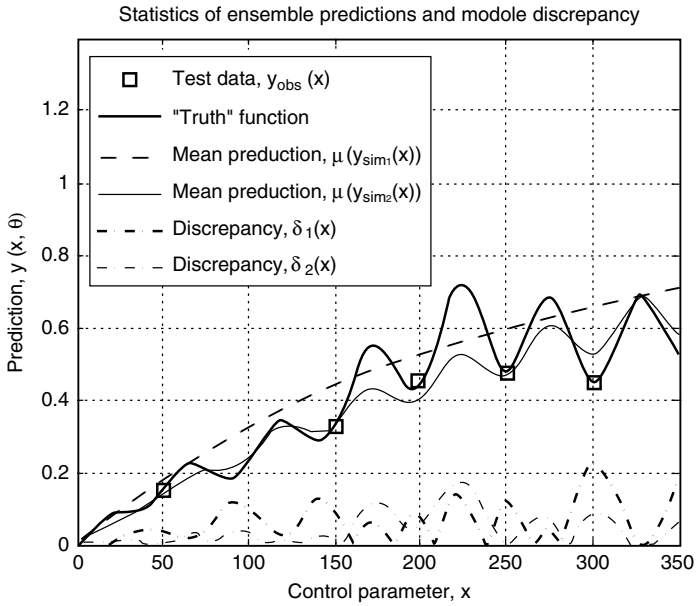

Figure 2: Comparison of Mean Predictions and Discrepancies ($\delta y1(x)$ is equal to 8.9% of the mean "truth", $\delta y2(x)$, is 4.6% of the mean "truth").

elements in ANSYS v.12. The Shell281 elements currently utilized in ANSYS v.12 were developed in response to a code verification study that brought into question the ability to properly model torsional bending [27], and recently verified [28] for their performance in bending, torsion, and modal analysis with closed form solutions applied to a hollow cylinder.

The blade used herein is 44 meters long with a representative geometry of a prototype wind turbine blade. The prototype blade dimensions are approximated from on-site measurements of a wind turbine blade located in Texas, as shown in Figure 3. Airfoil profiles available from the National Renewable Energy Laboratory are approximated from the measurements in the absence of design specifications for the cross-sections. The material composition of the prototype blade is modeled using material lay-ups similar to those given in Ref. [29]. First, a baseline FE model is created, in which the cross-section is modeled using orthotropic materials and a composite lay-up with bi-axial layers.

The prototype blade herein is modeled by defining different cross-sections at a specific distance from the root, hereby known as a station, as shown in Figure 4. The airfoil shape, twist of station, chord length, and distance from the root of the blade are specified at each station. The stations are then divided into material sections, to which different composite layers are assigned. The internal structure of the shear web is modeled by connecting delineation points through the airfoil cross-sections of the blade. To model the geometry accurately, nine stations with different material lay-ups are used. The shear web is idealized as having a constant thickness, with the height changing as the blade tapers. Five material sections are defined and represented in Figure 5: the root, the spar of the blade, the trailing edge, the leading edge, and the internal shear web that is not shown.

While generating the five alternative FE models, several assumptions about the material composition of the blade cross-section need to be established. In an effort to limit the changes solely due to model form error, equivalent material property values are maintained between the five models. Here, the bi-axial composite materials are defined using Young's Modulus, Shear Modulus, Poisson's ratio, density, thickness, and ply angle for rotation of the composite. To simplify the model from a bi-axial composite cross-section to uni-axial, the material

Figure 3: Measuring the wind turbine blade.

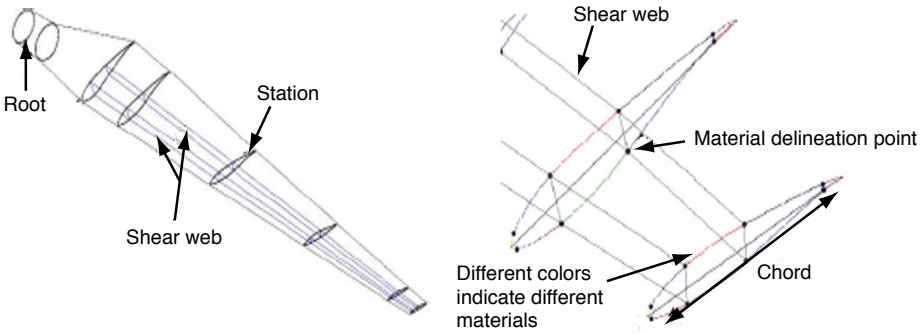

Figure 4: Wind turbine blade development in NuMAD.

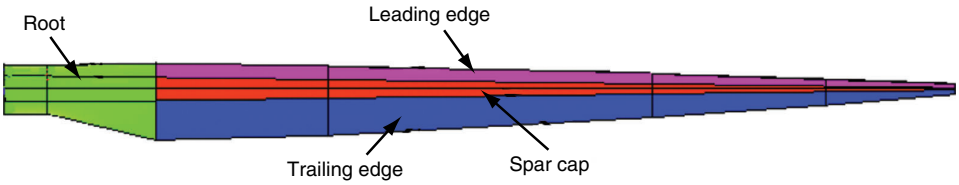

Figure 5: ANSYS model showing different sections of the blade.

properties for each layer are calculated from the transformation of local material properties onto a global axis. Changing the orientation of the local axis will affect the shear deformations [30], and resulting shear strengths that are responsible for distributing applied loads [31]. To assume an isotropic cross-section, equivalent material properties are produced so that the values used in the x-, y-, and z- directions are nominally identical. This however, will change the material stress-strain behavior and produce zero out of plane shear strain when the material undergoes plane-strain conditions [30]. To convert the model from a composite to a smeared cross-section, the rule of mixtures for composites, which has been shown to

Table 1: FE Models developed in ANSYS

FE model	Material properties	Lay-Up	Layer orientations	Input parameters	Computation time (sec)
Baseline	Orthotropic	Composite	Bi-Axial	90	99.45
Blade 1	Orthotropic	Composite	Uni-Axial	81	77.92
Blade 2	Isotropic	Smeared	N/A	45	45.69
Blade 3	Isotropic	Composite	N/A	36	88.13
Blade 4	Isotropic	Smeared	N/A	20	44.74

accurately model linear systems,[32] is applied and a characteristic Young's Modulus, Poisson's ratio and density are defined [33]. Smeared cross-sectional properties will create a uniform stress distribution, unlike when the stress can vary from layer to layer in composites [30], which by default ignores the in-plane deformations [34]. In addition, the rule of mixtures is not appropriate when there are a large number of voids in the composite [35]. These assumptions, applied to degrade the model sophistication, result in a decrease in the number of input parameters necessary to define the five alternative FE models (Table 1) and fulfill an overarching assumption necessary for this study: that the input parameters are known with certainty. Thus the predictive capabilities of the alternative models are degraded only due to the incompleteness and inaccuracy in which the underlying physics are represented.

As suggested in Table 1, the computation time necessary to complete a static analysis is dependent on the sophistication of the model. The Baseline blade requires 99.45 seconds, whereas Blade 4, modeled with the most simplifications, requires 44.74 seconds. Although there is a degradation in the sophistication of the physics used to model the cross sectional properties, there is more than a 50% reduction in computation time, which is sometimes necessary to make sensitivity analysis and calibration studies feasible.

3.2 Solution Verification with ANSYS

Solution verification is important to ensure that numerical errors have a negligible effect on the estimated model form error. Details of the mesh refinement study, which would be required by certification standards in the design of wind turbine blades [10], are provided for completeness.

The mesh convergence study is performed using static analysis in ANSYS v.12 by observing the stress at the blade root and the displacement of the blade tip due to point loads. To ensure that the global behavior of the blade is being compared, instead of local concentrations, the stress and displacements are approximated by averaging over nodes in the region of interest. Figure 6 shows six of the forty meshes used to perform the mesh

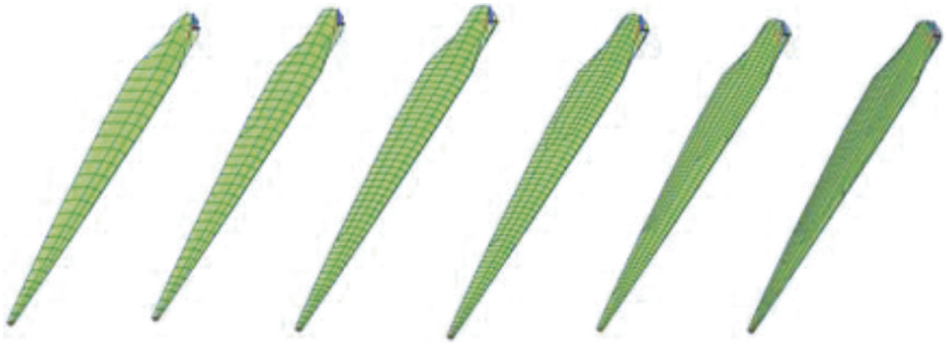

Figure 6: Six representative meshes in ANSYS (coarsest mesh with 62 elements and finest mesh with 10,663 elements).

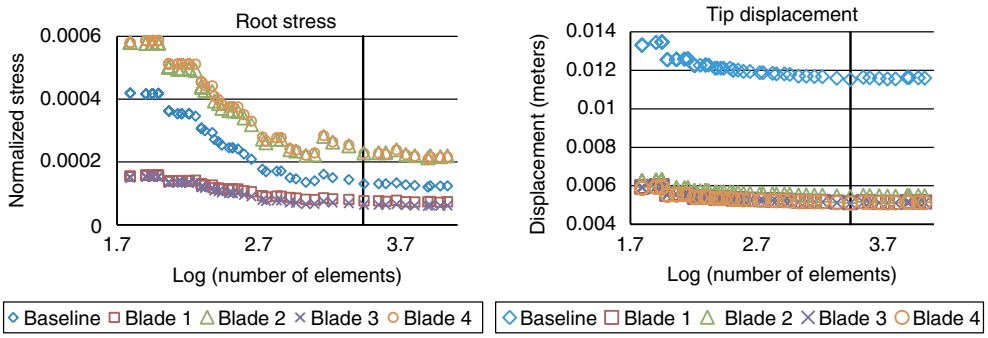

Figure 7: Mesh convergence of the root stress (Left) and tip displacement (Right).

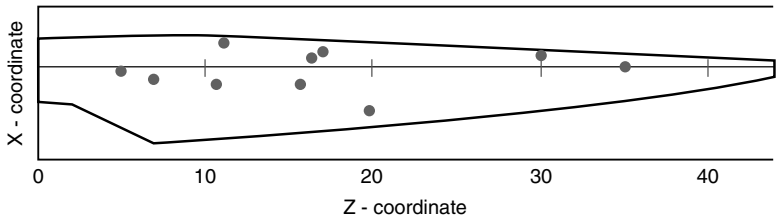

Figure 8: Blade profile with observed data points.

refinement study, and the convergence of the mesh is plotted in Figure 7 for all five blades. To quantify the solution uncertainty of the mesh refinement the "exact but unknown" solution, $y^{\text{Reference}}$ is calculated [36]. Previous experiments [37] showed that the natural frequency and damping for the first bending mode of a wind turbine blade has an average unit variability of 3.35%, thus, the chosen mesh size contains numerical errors consistent with a 1-σ bound of experimental variability. A mesh consisting of 2152 elements is chosen for the final FE model, indicated by the vertical black line in Figure 7. The solution error, inevitable due to the approximate nature of finite element analysis, is manifested into the estimates of model form error. However, the solution error due to tip displacement, calculated as 0.4%, will have a lower contribution to model form error than the root stress, calculated as 6.6%. These differences in solution error can be explained by the fact that asymptotic convergence was achieved at a coarser mesh size for the tip displacement.

4. INFERRING MODEL FORM ERROR FOR THE LESS COMPLEX BLADE MODELS

The baseline model described in Table 1 is used to generate reference data due to the highest level of sophistication provided. Reference data used herein is the blade tip displacement and root stress due to a concentrated point load applied at ten randomly chosen points on the surface of the blade. The tip displacement is calculated as the average of the nodal displacements at the tip of the blade, whereas the root stress is the root mean square of the nodal component stresses at the base of the blade. The location of each reference data point is controlled by the x and z coordinates of the blade. Thus, the x and z coordinates represent the control parameters, while all possible values of x and z represent the entire domain of applicability, which in this study, is the profile of the blade.

The reference data is used to determine the model incompleteness of the four blade models with lower sophistication. This is straightforward at the ten points where baseline data points are available. However, this discrete comparison at ten points only delivers a partial

knowledge about the model incompleteness. To achieve full knowledge the model form error must be quantified for the entire domain of applicability, i.e. all possible values of x and z. However, this requirement poses high demands on computational resources. Especially when the application of interest is not readily amenable to obtain a large number of physical experiments and the simulation model takes a considerable amount of time to complete. To eliminate these prohibitive demands on experimental and computational resources, we utilize the available reference data and train a GPM to represent the discrepancy bias. Therefore, the reference data from the baseline FE model is used to train a *discrepancy GPM* associated with the model (recall $\delta(x)$ in Eq. 1). The procedure is repeated for each of the four alternative modeling strategies.

For brevity, Figure 9 presents the results for Blade 4 only. Figure 9a illustrates the disagreement between the model predictions of Blade 4 and the reference data points provided from the baseline model. The trained *discrepancy GPM* is non-deterministic in nature, therefore error bars are used to represent the bias-corrected predictions. For all ten data points, the reference data falls within the range of bias-corrected predictions, increasing confidence in the mathematical representation provided by the GPM. The discrepancy, taken as the difference between model predictions and bias-corrected predictions, are plotted in Figure 9b, for the ten locations of reference data.

To obtain a holistic representation of discrepancy, the root stress and tip displacement are predicted when the concentrated load is applied anywhere on the blade surface, i.e. over the entire domain of applicability. When plotted, these predictions form a surface in a three-dimensional plane, as shown in Figure 10. The volume between the model predictions before and after bias-correction, henceforth referred to as *discrepancy volume,* yields a convenient metric to estimate the level of model incompleteness. The discrepancy volumes calculated for each blade model are reported in Table 2 for both tip displacement and root stress.

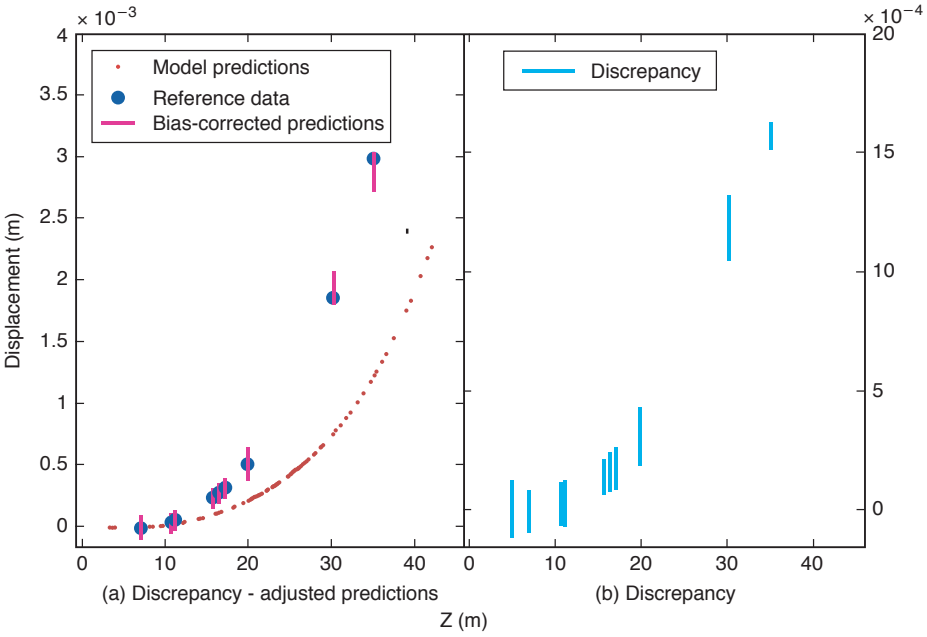

Figure 9: Simulator outputs.

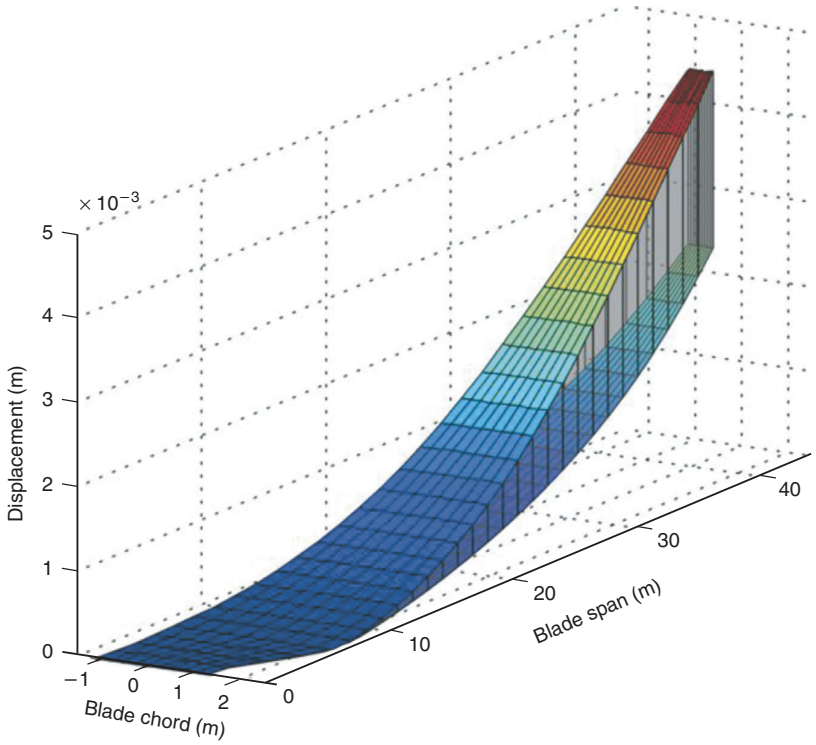

Figure 10: Bias-corrected predictions (top) and calibrated predictions (bottom).

Table 2: Discrepancy volume of the blade models

FE model	Volume due to tip displacement	Volume due to root stress
Blade 1	0.01953	0.00032
Blade 2	0.01762	0.00073
Blade 3	0.01964	0.00040
Blade 4	0.01954	0.00058

The resulting discrepancy volumes can be used as a convenient metric to quantify the *model form error* of the alternative FE models and can be described by the underlying physics. The most significant effect on the discrepancy volume for the *tip displacement* occurs when the orientation of the local axis is modified from the baseline blade, with bi-axial layers, to Blade 1, with uni-axial layers. Once this assumption is applied, there is a negligible change in discrepancy volumes of the four alternative models. This behavior can be described by considering the global stiffness of the blade, which stays consistent for the four alternative models. In comparison, the degraded physics affects the behavior of the cross-sectional areas, producing significant changes in the discrepancy volumes produced for the *root stress*. The discrepancy volume for the root stress is consistent with the lay-up used in the model (Table 1): Blades 1 and 3 were modeled using composite cross sections, and Blades 2 and 4 were modeled using smeared cross sections.

5. QUANTIFYING PREDICTIVE MATURITY OF ALTERNATIVE NUMERICAL MODELS

Recently, a science-based, holistic metric to quantify the predictive capability of simulation models, the predictive maturity index (PMI) was proposed [38]. The quantitative nature of the PMI sets it apart from the qualitative methods that have been proposed in the past [39, 40]. In

this section, we describe our use of PMI to compare the five alternative models introduced in Section 3.

Many earlier methods considered the goodness of fit of the model predictions to available test data [39, 40]. However, good fidelity to test data depicts an incomplete picture regarding the model predictiveness. This is especially true in cases of over-fitting, in which a model may exhibit a high fidelity to data while producing predictions with low accuracy at untested settings. Furthermore, it can be shown that the fidelity to available test data and the predictive capability of a model have an antagonistic relationship [41]. While model form error, defined in Section 2.2, is capable to quantify the incompleteness of the model, the PMI goes a step further in quantifying the predictive maturity.

Three aspects of the simulation model are considered when defining the PMI: *coverage*, *complexity* of the model, and the *overall level of accuracy*. *Coverage* quantifies how well the available test data covers the domain of applicability. In this study, the coverage is quantified by finding the ratio of the convex hull of the reference data to the area of the entire domain of applicability. *Complexity* is a measure of the level of detail that is used to model the physics, quantified by the number of calibration parameters associated with each model. With everything else equal, if the value used to define complexity increases, the PMI should decrease. This decrease is because a model with an infinite number of parameters is prone to over-fitting; it has an excellent ability to reproduce experimental data but no predictive capability. The *overall level of accuracy* is quantified using model form error, calculated in the previous section. Not to be confused with goodness of fit, the overall level of accuracy considers the differences between the simulated data and reference data that cannot be accounted for by varying the calibration parameters. The formulation for the PMI as proposed by Ref. [38] is given below:

$$\mathrm{PMI} = \eta_c \times \left(\frac{N_R}{N_K}\right)^{\gamma_1} \times \left(1-\delta_s\right)^{\gamma_2} \times e^{\left(1-\eta_c^2\right)^{\gamma_3}\delta_s^2} \tag{2}$$

where η_c is the coverage, N_R represents the sophistication of the state of the art, N_K is the sophistication of the model that one is assessing, and δ_s is the measure of goodness of fit [38]. In Eqn. 2, the γ values are user defined coefficients used to weigh the effects of these contributions to predictive maturity.

For the five alternative models investigated herein coverage remains constant at 0.4 because the control parameters for the ten reference data points are identical for each blade. In this study, complexity is quantified by using the number of calibration parameters associated with each model, as reported in Table 1. The overall level of accuracy is obtained by scaling the model form error such that the values vary between 0 and 1. Table 3 shows the values obtained for complexity and overall level of accuracy.

By definition, a PMI of 1 means that the model has perfect predictive maturity, and a PMI of 0 means that the model has zero predictive maturity. The values of PMI should be used in a relative sense as a comparison between different codes, not as an absolute value. As seen in Table 4, the PMI calculated for each model varies significantly, with the highest assigned to Blade 4 and lowest assigned to Blade 1. This is expected because even though Blade 1 has the largest number of calibration parameters, there is no realized gain in predictive capability from the added complexity of the model.

The PMI metric is able to incorporate the trade-offs between the number of parameters used in each model and the discrepancy bias associated with each model. While a more sophisticated model generally has the potential to capture the underlying physics principles better, it cannot be assumed by default that such a model has greater predictive capability.

Table 3: PMI calculated for each model ($\gamma_1 = 0.5$ and $\gamma_2 = 0.25$, and $\gamma_3 = 10$)

FE model	Complexity	Tip displacement accuracy	Root stress accuracy
Blade 1	0.90	0.391	0.224
Blade 2	0.50	0.352	0.510
Blade 3	0.40	0.393	0.276
Blade 4	0.22	0.391	0.402

Table 4: PMI calculated for each model ($\gamma_1 = 0.5$ and $\gamma_2 = 0.25$, and $\gamma_3 = 10$)

FE model	Tip displacement PMI	Root stress PMI
Blade 1	44.6%	47.2%
Blade 2	60.7%	56.8%
Blade 3	66.8%	69.7%
Blade 4	89.7%	89.3%

It is also important to note that the two smeared FE models, Blades 2 and 4 required 44% less computation time than the baseline Blade model. The reduction in computational demands combined with the decreased number of calibration parameters and higher PMI values make FE models that simplify the modeled cross-sections of wind turbine blades potentially attractive to implement.

6. CONCLUSIONS

The predictive capabilities associated with alternative modeling strategies are investigated through a prototype FE model of a 44-meter prototype wind turbine blade. Five alternative models of wind turbine blades are developed and their predictiveness is compared. The blade model with highest complexity required 90 calibration parameters, whereas the least complex model required only 20 calibration parameters. *Discrepancy GPMs* are compared to simulated data from the blade models to estimate the discrepancy bias across the entire domain of applicability.

The initial simplification of rotating composite layers to develop a material cross-section with composite layers oriented in the same direction is observed to have the greatest effect on the calculated discrepancy bias. This produced a comparable discrepancy bias estimated for the four alternative FE models. The blade model with the lowest number of input parameters was found to have the highest PMI, which can be explained by the fact that increased model sophistication was not able to provide significant gains in predictiveness.

The quantitative nature of the PMI captures the trade-off between the number of parameters necessary for each model and the discrepancy bias associated with these models. Therefore, PMI is useful for comparing alternative modeling strategies and defending the level of sophistication used in an FE model. Moreover, the PMI would mitigate issues that may arise from over-fitting because it takes into account the predictive capabilities and not just the fidelity to test data.

Even though the lack of experimental data is a shortcoming of the present study, the objective, quantitative and repeatable procedures presented herein are generally applicable in cases where experimental data is available. Even though only the material cross section is considered, other commonly applied assumptions that are applied in wind turbine blade modeling could be investigated. Furthermore, in this study the calibration parameters are kept at their nominal values; however, the proposed approach is amenable to incorporate parameter calibration. Even though not emphasized in this manuscript, it should be noted that a thorough sensitivity analysis of the input parameters should also be carried out prior to

parameter calibration or bias-correction activities. To reiterate, only the parameters that have a noticeable influence on the output of interest should be considered during the PMI calculations.

Using model form error and PMI to create quantifiable metrics for the predictive capabilities of FE models has the potential to aid in future attempts to model wind turbine blades by scientifically defending the level of complexity necessary for simulations of wind turbine blades. Such quantitative metrics are important to the future of modeling and simulation of wind turbine blades, as the computational cost can be reduced if a less complex model can be found to adequately model wind turbine blade vibrations.

ACKNOWLEDGEMENTS

The authors wish to express their gratitude to Jean-Paul Cane, of Rope Partner, Inc. for providing the on-site measurements and photos of the prototype wind turbine blade. Many thanks to Brian Williams from Los Alamos National Laboratory for providing guidance in surrogate models and GPMSA analysis.

REFERENCES

[1] Lindenberg, S., Smith, B., O'Dell, K., and DeMeo, E., 20% wind energy by 2030: increasing wind energy's contribution to US electricity supply, DOE/GO-102008-2567, 2008.

[2] Veers, P.S., Ashwill, T.D., Sutherland, H.J., Laird, D.L., Lobitz, D.W., Griffin, D.A., Mandell, J.F., Musial, W.D., Jackson, K., Zuteck, M., Miravete, A., Tsai, S.W. and Richmond, J.L., Trends in the Design, Manufacture and Evaluation of Wind Turbine Blades, *Wind Energy*, 2003, 6(3), 245–259.

[3] o Griffith, D.T., Carne, T.G., and Paquette, J.A., Modal testing for validation of blade models, *Wind Engineering*, 2008, 32(2), 91-102.

[4] Ashwill, T., Blade Technology Innovations for Utility-Scale Turbines, SAND2006-4941C, Sandia National Laboratories, Albuquerque, NM, 2006.

[5] Ashwill, T. and Laird, D., Concepts to facilitate very large blades, *Proceedings, ASME/AIAA Wind Energy Symposium*, 2007, Reno, NV.

[6] Paquette, J.A. and Veers, P.S., Increased strength in wind turbine blades through innovative structural design, *Proceedings, European Wind Energy Conference*, 2007, Milan, Italy.

[7] Resor, B., Paquette, J., Laird, D. and Griffith, D.T., An evaluation of wind turbine blade cross section analysis techniques, *AIAA/ASME/ASCE/AHS/ASC Structures, Structural Dynamics, and Materials Conference*, 2010, Orlando, FL.

[8] Ghoshal, A., Sundaresan, M.J., Schulz, M.J. and Pai, P.F., Structural health monitoring techniques for wind turbine blades, *Journal of Wind Engineering and Industrial Aerodynamics*, 2000, 85(3), 309-324.

[9] Jensen, F.M., Falzon, B.G., Ankersen, J. and Stang, H., Structural testing and numerical simulation of a 34 m composite wind turbine blade, *Composite Structures*, 2006, 76(1-2), 52–61.

[10] Det Norske Veritas, Design and Manufacture of Wind Turbine Blades, Offshore and Onshore Wind Turbines, October 2010.

[11] Jackson, K.J., Zuteck, M.D., van Dam, C.P., Standish, K.J. and Berry, D., Innovative design approaches for large wind turbine blades, *Wind Energy*, 2004, 8(2), 141–171.

[12] Adams, D., White, J., Rumsey, M. and Farrar, C., Structural health monitoring of wind turbines: method and application to a HAWT, *Wind Energy*, 2011, 14(4), 603–623.

[13] Simmermacher, T., James, G.H. and Hurtado, J.E., Structural health monitoring of wind turbines, *International workshop on structural health monitoring*, 18–20 September 1997, Stanford, CA, USA.

[14] o Mollineaux, M.G., Van Buren, K.L., Hemez, F.M., and Atamturktur, S., Simulating the dynamics of wind turbine blades: part I, model development and verification, *Wind Energy*, 2012, doi: 10.1002/we.1519.

[15] Bazilevs, Y., Hsu, M.C., Kiendl, J., Wuchner, R. and Bletzinger, K.U., 3D simulation of wind turbine rotors at full scale Part II: Fluid-structure interaction modeling with composite blades, *International Journal for Numerical Methods in Fluids*, 2011, 65(1–3), 236–253.

[16] Zhang, J.P. and Pan, L.L., Three-dimensional modeling and aeroelastic coupling analysis for the wind turbine blade, *World Non-Grid-Connected Wind Power and Energy Conference*, 24–26 September 2009, Nanjing, China.

[17] Kennedy, M. and O'Hagan, A., Predicting the output from a complex computer code when fast approximations are available, *Biometrika*, 2000, 87(1), 1–13.

[18] Bechly, M.E. and Clausen, P.D., Structural design of a composite wind turbine blade using finite element analysis, *Computers & Structures*, 1997, 63(3), 639–646.

[19] Jensen, F., Falzon, B.G., Ankersen, J. and Stang, H., Structural testing and numerical simulation of a 34 m composite wind turbine blade, *Composite Structures*, 2006, 76(1–2), 52–61.

[20] Malcolm, D.J. and Laird, D.L., Modeling of blades as equivalent beams for aeroelastic analysis, *Proceedings of the AIAA/ASME Wind Energy Symposium*, 2003, Reno, NV.

[21] Mikkelsen, L.P., Sorensen, K.D. and Jensen, H.M., A smeared-out material model predicting compressive failure of composites, *NAFEMS NORDIC Seminar*, 2010.

[22] Alpay, S., Barut, A. and Madenci, E., An efficient modeling approach for dynamic simulation of wind turbine blades, *AIAA/ASME/ASCE/AHS/ASC Structures, Structural Dynamics, and Materials Conference*, 2010.

[23] Murtagh, P., Basu, B. and Broderick, B., Mode acceleration approach for rotating wind turbine blades, *Proceedings of the Institution of Mechanical Engineers, Part K: Journal of Multi-body Dynamics*, 2004, 218(3), 159–167.

[24] Pardo, D. and Branner, K., Finite element analysis of the cross-section of wind turbine blades; a comparison between shell and 2D-solid models, *Wind Engineering*, 2005, 29(1), 25–32.

[25] Higdon, D., Gattiker, J., Williams, B. and Rightley, M., Computer model calibration using high-dimensional output, *Journal of the American Statistical Association*, 2008, 103(482), 570–583.

[26] Hemez, F.M. and Atamturktur, H.S., "Prediction with quantified uncertainty of temperature and rate dependent material behavior," *11th AIAA Non-Deterministic Approaches Conference*, 2009.

[27] Laird, D.L., Montoya, F.C. and Malcolm, D.J., Finite element modeling of wind turbine blades, *43rd AIAA Aerospace Science Meeting and Exhibit*, 2005.

[28] Mollineaux, M., Van Buren, K. and Hemez, F., Simulating the dynamics of wind turbine blades: part I, model development and verification, *13th AIAA Non-deterministic Approaches Conference*, 2011.

[29] Berry, D. and Ashwill, T., Design of 9-meter carbon-fiberglass prototype blades: CX-100 and TX-100, Sandia National Laboratories, 2007.

[30] Kollár, L.P. and Springer, G.S., Mechanics of *Composite Structures*, Cambridge University Press, 2003.

[31] Mandell, J.F., Samborsky, D.D., Combs, D.W., Scott, M.E. and Cairns, D.S., Fatigue of composite material beam elements representative of wind turbine blade substructure, National Renewable Energy Laboratory, 1998.

[32] Kouznetsova, V., Brekelmans, W.A.M. and Baaijens, F.P.T., An approach to micro-macro modeling of heterogeneous materials, *Computational Mechanics*, 2001, 27, 37–48.

[33] Tsai, S. and Hahn, H.T., *Introduction to Composite Materials*, Westport, Conn., 1980.

[34] Syed, K.A.N., *Analysis of hat-sectioned reinforced composite beams including thermal effects*, PhD Thesis, The University of Texas at Arlington, 2006.

[35] Sarkar, B.K., Estimation of composite strength by a modified rule of mixtures incorporating defects, *Bulletin of Material Science*, 1998, 21(4), 329–333.

[36] Roache, P.J., *Verification and Validation in Computational Science and Engineering*, Hermosa Publishers, Albuquerque, NM, 1998.

[37] Griffith, D.T. and Carne, T.G., Experimental uncertainty quantification of modal test data, *25th International Modal Analysis Conference*, 2007.

[38] Hemez., F.M., Atamturktur, H.S. and Unal, C., Defining predictive maturity for validated numerical simulations, *Computers & Structures*, 2010, 88(7–8), 497–505.

[39] Balci, O., Adams, R.J., Myers, D.S. and Nance, R.E., Credibility assessment: a collaborative evaluation environment for credibility assessment of modeling and simulation applications, *Proceedings of the 34th Conference on Winter Simulation: Exploring New Frontiers*, 2002.

[40] Harmon, S.Y. and Youngblood, S.M., A proposed model for simulation validation process maturity, *The Journal of Defense Modeling and Simulation: Applications, Methodology, Technology*, 2005, 2(4), 179–190.

[41] Hemez, F.M. and Ben-Haim, Y., The good, the bad, and the ugly of predictive science, *4th International Conference on Sensitivity Analysis of Model Output*, 2004.